Electronic Supplementary Information

New Strategy to Prepare Surface-Enhanced Raman Scattering-Active Substrates by Electrochemical Pulse Deposition of Gold Nanoparticles

Fu-Der Mai[a], Ting-Chu Hsu[b], Yu-Chuan Liu[*a], Kuang-Hsuan Yang[c] and Bo-Chuen Chen[c]

[a] *Department of Biochemistry, School of Medicine, College of Medicine, Taipei Medical University, No. 250, Wu-Hsing St., Taipei 11031, Taiwan. Fax: 886-2-27356689; Tel: 886-2-27361661 ext 3155; E-mail: liuyc@tmu.edu.tw*

[b] *General Education Center, Vanung University, Chung-Li City, Taiwan.*

[c] *Department of Chemical and Materials Engineering, Vanung University, Chung-Li City, Taiwan.*

Chemical Reagents

Electrolytes of KCl and R6G reagents (p.a. grade) were purchased from Acros Organics and used as received without further purification. All of the solutions were prepared using deionized 18.2 MΩ cm water provided from a MilliQ system.

Electrochemical preparation of Au-containing complexes in solution

All the electrochemical experiments were performed in a three-compartment cell at room temperature (24^{o}C) and were controlled by a potentiostat (model PGSTAT30, Eco Chemie). A sheet of gold with bare surface area of 4 cm^2, a 2 ×4 cm^2 platinum sheet, and KCl-saturated silver-silver chloride (Ag/AgCl) were employed as the working, counter and reference electrodes, respectively. Before the treatment of oxidation-reduction cycles (ORCs), the gold electrode was mechanically polished (model Minimet 1000, Buehler) successively with 1 and 0.05 μm of alumina slurry to a mirror finish. Then the electrode was cycled in a deoxygenated 0.1 M KCl aqueous solution (40 mL) from -0.28 to +1.22 V vs Ag/AgCl at a scan rate of 500 mV/s for 200 scans. The durations at the cathodic and anodic vertices are 10 and 5 s, respectively. After the ORCs treatment, Au- and Cl-containing complexes were produced in the solution, as reported in our previous study.[1]

Sonoelectrochemical preparation of SERS-active Au NPs on Pt substrate

Immediately, the working electrode of gold was replaced by a platinum substrate with a bare surface area of 0.238 cm^2 in the same solution. Here the platinum substrate was chosen because it is inert in the following experiments. Then a cathodic overpotential of 0.6 V and different anodic overpotentials from open circuit potential (OCP) of ca.

0.81 V vs Ag/AgCl were applied in turn under sonication to prepare effectively SERS-active Au NPs on the Pt substrate. Also, the ratio of reaction times of cathodic deposition to anodic dissolution of Au NPs was investigated for obtaining most effective SERS effect. In applying the cathodic overpotential for pulse deposition of Au NPs, the total accumulated deposition time is 60 s for every experiment. After this deposition of SERS-active Au NPs, the platinum substrate was rinsed throughout with deionized water, and finally dried in a dark vacuum-dryer for 1 h at room temperature for subsequent use. The ultrasonic treatment was performed by using an ultrasonic generator (model XL2000, Microson) and operated at 20 kHz with a barium titanate oscillator of 3.2 mm diameter to deliver a power of 80 W. The distance between the barium titanate oscillator rod and the electrode is kept at 5 mm.

Adsorption of R6G on SERS-active Au NPs deposited on Pt substrate

For SERS measurements, the prepared SERS-active Au NPs-containing platinum substrates were incubated in 2×10^{-5} M R6G aqueous solutions for 30 min. Then the substrates were rinsed throughout with deionized water, and finally dried in a dark vacuum-dryer for 1 h at room temperature for subsequent test.

Characterization of SERS-active Au NPs deposited on Pt substrate

The surface morphologies of Au NPs-containing platinum substrates were examined by scanning electron microscopy (SEM, model S-4700, Hitachi). For X-ray diffraction (XRD) measurements, instrument of ARL X'TRA Thermo was used. A scan rate of 5^{o}/min was employed. For high resolution X-ray photoelectron spectroscopy (HRXPS) measurements, a ULVAC PHI Quantera SXM spectrometer with monochromatized Al K_{α} radiation, 15 kV and 25 W, and an energy resolution of 0.1 eV was used. To avoid the interferential signals from the substrate, an arrangement of tilt 15^{o} geometry between X-ray and samples was used in measurements. To compensate for surface charging effects, all HRXPS spectra are referred to the C 1s neutral carbon peak at 284.8 eV. Surface chemical compositions were determined from peak-area ratios corrected with the approximate instrument sensitivity factors. Raman spectra were obtained (Renishaw InVia Raman spectrometer) by using a confocal microscope employing a He-Ne laser operating at 632.8 nm with an output power of 1 mW on the sample. A 50x, 0.75 NA Leica objective was used to focus the laser light on the samples. The laser spot size is ca. 1~2 μm. A thermoelectrically cooled charge-coupled device (CCD) 1024 x 256 pixels operating at -60 ^{o}C was used as the detector with 1 cm^{-1} resolution. All spectra were calibrated with respect to silicon wafer at 520 cm^{-1}. In measurements, a 90^{o} geometry was used to collect the scattered radiation. A holographic notch filter was used to filter the excitation line

from the collected light. The acquisition time for each measurement was 10 s. Replicate measurements of three times on different areas were made to verify the spectra were a true representation of each experiment. The relative standard deviation is within 5 % based on the strongest band intensity of R6G on the Raman spectrum. Also, different batches of the as synthesised substrates were measured by using the same conditions for three times. The relative deviation from the average value is less than 5 % for an individual sample based on the strongest band intensity of R6G on the Raman spectrum.

Supplemental Figures and Corresponding Discussions

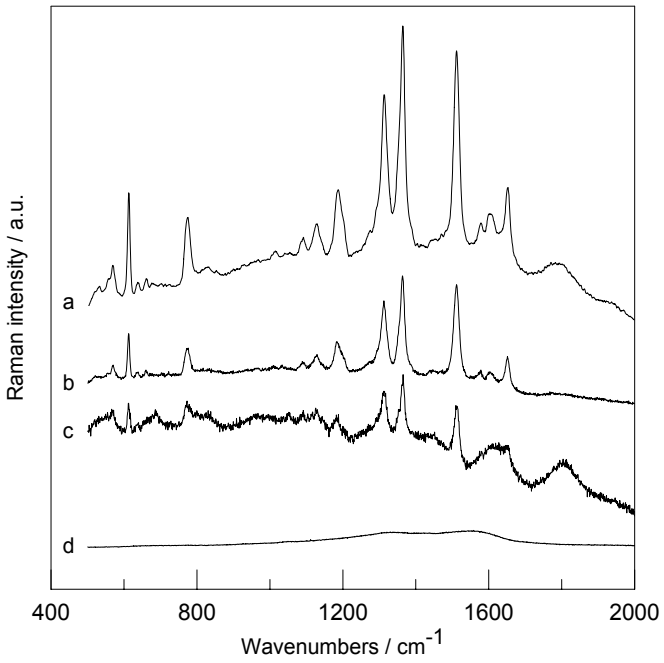

Fig. S1. SERS spectra of R6G with different concentrations adsorbed on Au NPs-deposited Pt substrate prepared by sonoelectrochemical deposition-dissolution cycles under a cathodic overpotential of 0.6 V and an anodic overpotential of 0.2 V from OCP with a ratio of reaction times of deposition to dissolution of Au NPs to be 0.2. Spectra a~c represent the concentrations of R6G being 2×10^{-5}, 2×10^{-9} and 2×10^{-12} M, respectively; spectrum d represents the blank Raman spectrum of the Au NPs-deposited Pt substrate without R6G.

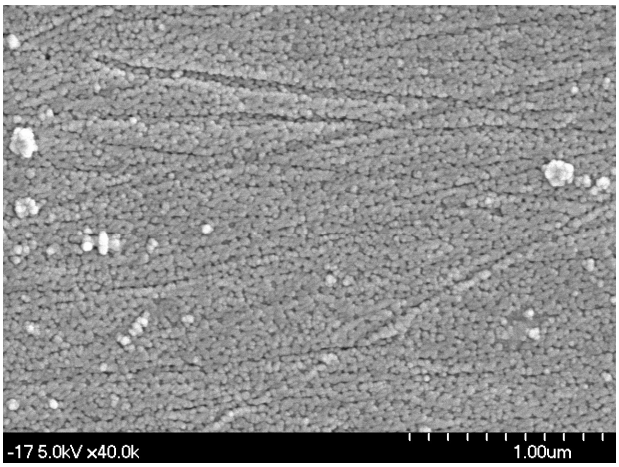

(a)

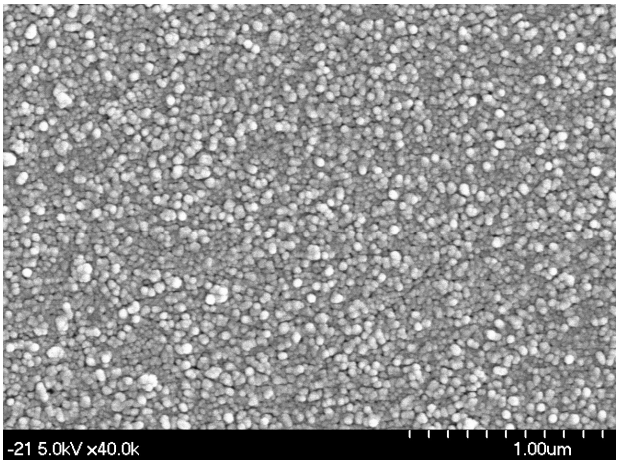

(b)

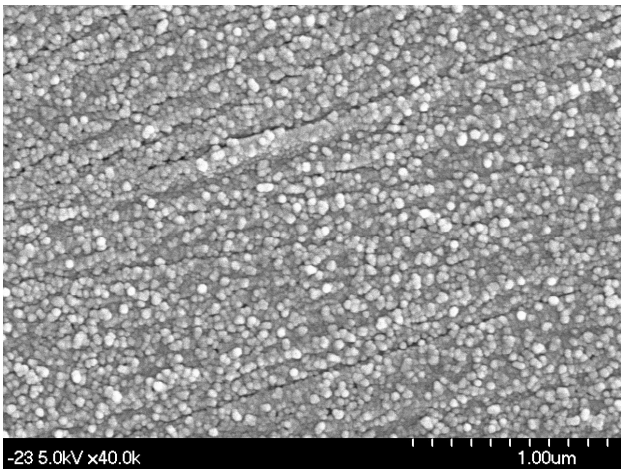

(c)

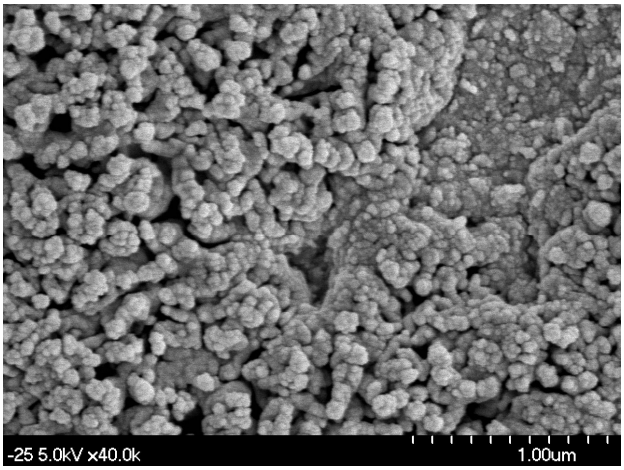

(d)

Fig. S2. SEM images of different Au NPs-deposited Pt substrates prepared by sonoelectrochemical deposition-dissolution cycles under a cathodic overpotential of 0.6 V and different anodic overpotentials from OCP with a ratio of reaction times of deposition to dissolution of Au NPs to be 0.2: (a) anodic overpotential of 0 V; (b) anodic overpotential of 0.2 V; (c) anodic overpotential of 0.4 V; (d) anodic overpotential of 0.6 V.

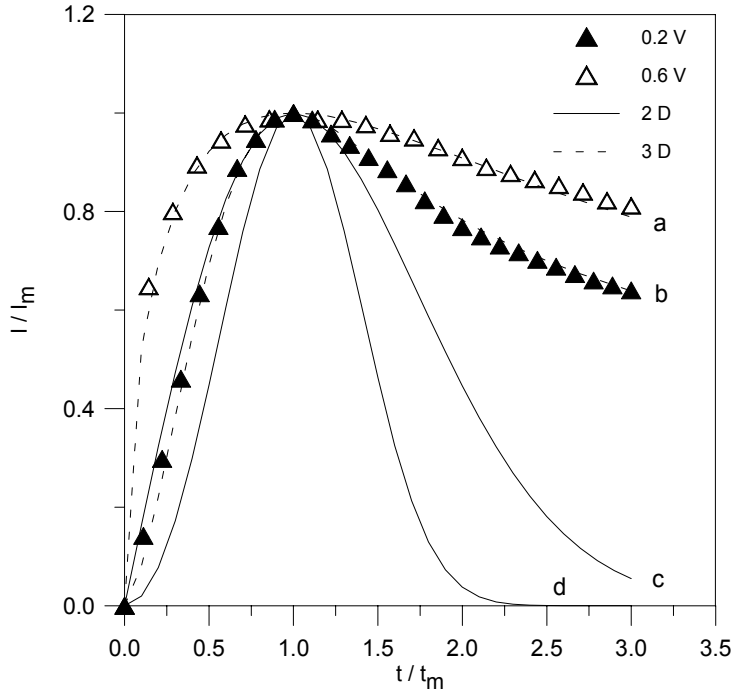

Fig. S3. Dimensionless plots of I-t curves for different Au NPs-deposited Pt substrates prepared by sonoelectrochemical deposition-dissolution cycles under a cathodic overpotential of 0.6 V and different anodic overpotentials of 0.2 V (solid triangle) and 0.6 V (hollow triangle) from OCP with a ratio of reaction times of deposition to dissolution of Au NPs to be 0.2, as compared with theoretical models for nucleation. Curves a and b represent 3D instantaneous and progressive models (dashed lines), respectively. Curves c and d represent 2D instantaneous and progressive models (solid lines), respectively.

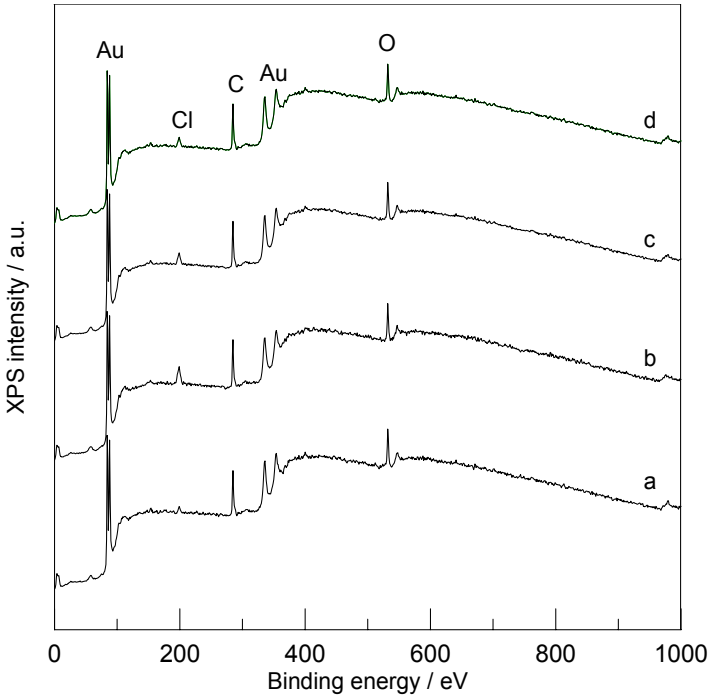

Fig. S4. HRXPS survey spectra of different Au NPs-deposited Pt substrates prepared by sonoelectrochemical deposition-dissolution cycles under a cathodic overpotential of 0.6 V and different anodic overpotentials from OCP with a ratio of reaction times of deposition to dissolution of Au NPs to be 0.2: (a) anodic overpotential of 0 V; (b) anodic overpotential of 0.2 V; (c) anodic overpotential of 0.4 V; (d) anodic overpotential of 0.6 V.

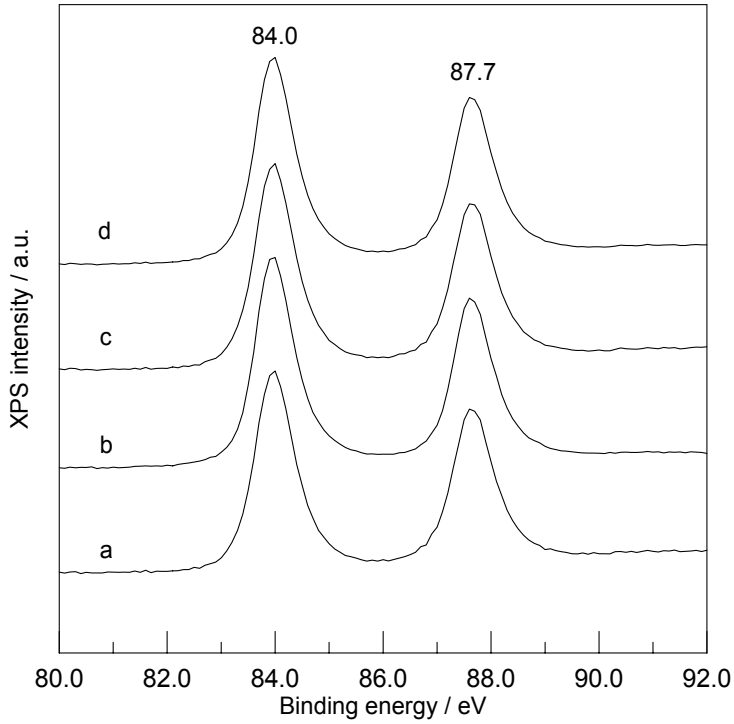

Fig. S5. HRXPS Au $4f_{7/2\text{-}5/2}$ core-level spectra of different Au NPs-deposited Pt substrates prepared by sonoelectrochemical deposition-dissolution cycles under a cathodic overpotential of 0.6 V and different anodic overpotentials from OCP with a ratio of reaction times of deposition to dissolution of Au NPs to be 0.2: (a) anodic overpotential of 0 V; (b) anodic overpotential of 0.2 V; (c) anodic overpotential of 0.4 V; (d) anodic overpotential of 0.6 V.

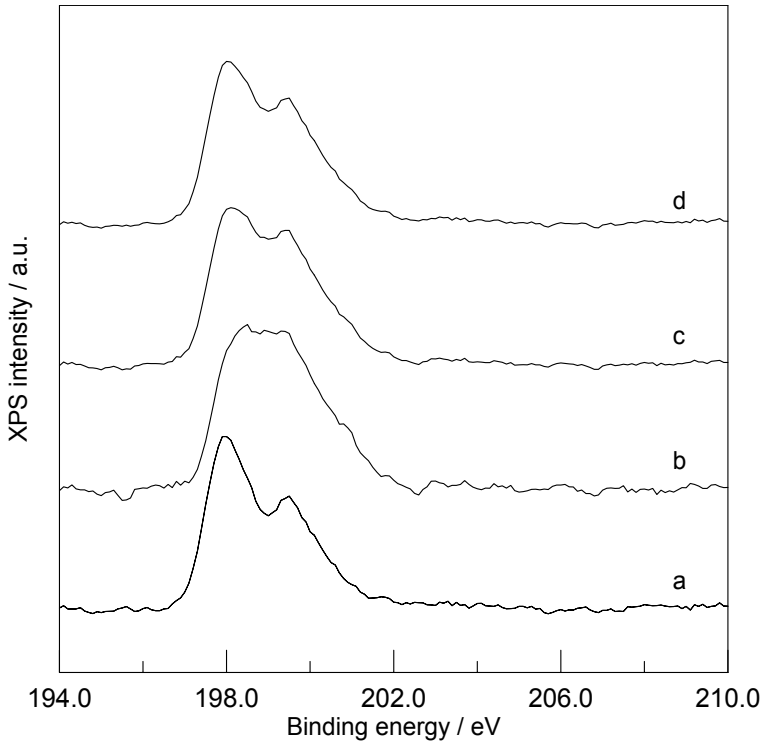

Fig. S6. HRXPS Cl 2p core-level spectra of different Au NPs-deposited Pt substrates prepared by sonoelectrochemical deposition-dissolution cycles under a cathodic overpotential of 0.6 V and different anodic overpotentials from OCP with a ratio of reaction times of deposition to dissolution of Au NPs to be 0.2: (a) anodic overpotential of 0 V; (b) anodic overpotential of 0.2 V; (c) anodic overpotential of 0.4 V; (d) anodic overpotential of 0.6 V.

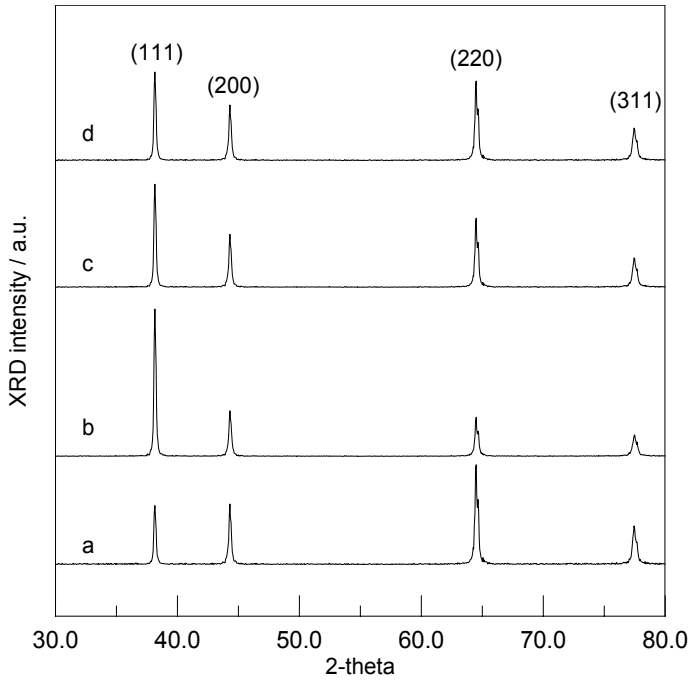

Fig. S7. XRD patterns of different Au NPs-deposited Pt substrates prepared by sonoelectrochemical deposition-dissolution cycles under a cathodic overpotential of 0.6 V and different anodic overpotentials from OCP with a ratio of reaction times of deposition to dissolution of Au NPs to be 0.2: (a) anodic overpotential of 0 V; (b) anodic overpotential of 0.2 V; (c) anodic overpotential of 0.4 V; (d) anodic overpotential of 0.6 V.

As shown in Fig. S1, the spectra resolutions are reduced with diluting the concentrations of the target analytes, as expected. Spectrum d of Fig. S1 represents the blank Raman spectrum of the Au NPs-deposited Pt substrate without R6G. As comparing spectrum c with spectrum d, it was found that additional characteristic R6G peaks still clearly appear at ca. 1313, 1363 and 1511 cm^{-1}. Thus, the LOD for R6G adsorbed on the Au NPs-deposited Pt substrate proposed in this work was decided to be ca. 2×10^{-12} M.

To further realize the influences of preparation conditions in DDCs methods on the corresponding SERS performances HRXPS analyses were performed to examine the surface components formed on the Au NPs-deposited Pt substrates. Fig. S3 shows the HRXPS survey spectra of Au NPs-deposited Pt substrates prepared by applying different anodic overpotentials at a fixed ratio of 0.2 of cathodic deposition time to

anodic dissolution time. The main signals of Au and Cl are clearly shown in these spectra. Generally, the signals of C and O are unavoidably present in HRXPS spectra even though the samples don't contain these two components. Basically, these four spectra are similar. The only noticeable phenomena are different intensities of Cl signals. Further analyses of surface chemical compositions show that the contents of Cl are 3.5, 8.9, 6.3 and 4.9 mol % for the Au NPs-deposited Pt substrates prepared by applying anodic overpotentials of 0, 0.2, 0.4 and 0.6 V, respectively. Interestingly, these contents of Cl are proportional to their corresponding SERS intensities, as demonstrated in Fig. 2 (in the text). This phenomenon was also observed in other SERS study of Ag system of our previous report.[2] As reported in the literature,[3-5] anions-contained complexes of metals, which were distinguishable from bulk metals, were easily formed during the electrochemical deposition. It was also found that the SERS activity is much more stable when the constituents of the complex are simultaneously present.[6] Furthermore, it was believed that the SERS effect chiefly comes from the corresponding complex formed at the interface of roughened metal.[4] In this electrochemical DDCs method, negatively charged chloride ions, as discussed later, are the main anions in the anions-contained complexes of gold. They are contributive to the increased SERS effects.

Fig. S5 displays the HRXPS Au spectra observed on Au NPs-deposited Pt substrates prepared by applying different anodic overpotentials at a fixed ratio of 0.2 of cathodic deposition time to anodic dissolution time. Basically, these four spectra are almost identical with the doublet peaks located at 84 and 87.7 eV, which can be assigned to Au(0).[7] It means that the Au NPs deposited on Pt substrates are all elemental states under applying different anodic overpotentials in DDCs processes. Fig. S6 show the HRXPS Cl 2p core-level spectra of Au NPs-deposited Pt substrates prepared by applying different anodic overpotentials at a fixed ratio of 0.2 of cathodic deposition time to anodic dissolution time. Further analyses indicate that the main peaks of the chloride-containing Au NPs formed on Pt substrates prepared by applying different anodic overpotentials are located mostly in the region between 197 and 202 eV. These chloride peaks can be assigned to Cl (-1).[1] However, further deconvoluting the peaks on the spectra and comparing the different subpeaks under different preparation conditions can reveal interesting results (data not shown here). In the HRXPS Cl 2p deconvolution in the region between 196 and 203 eV, the three component peaks are located at ca. 197.8, 199.4 and 200.5 eV with equal values of full width at half-maximum (FWHM) to the utmost in each deconvolution. The contents of the component peak at 197.8 eV are 55, 30, 42 and 52% for Au NPs-deposited Pt substrates prepared by applying anodic overpotentials of 0, 0.2, 0.4 and 0.6 V, respectively. The contents of the component peak at 199.4 eV are 23, 36,

30 and 25% for Au NPs-deposited Pt substrates prepared by applying anodic overpotentials of 0, 0.2, 0.4 and 0.6 V, respectively. The contents of the component peak at 200.5 eV are 22, 34, 28 and 23% for Au NPs-deposited Pt substrates prepared by applying anodic overpotentials of 0, 0.2, 0.4 and 0.6 V, respectively. As comparing these contents of the component peaks of Cl for Au NPs-deposited Pt substrates prepared by applying different anodic overpotentials with their corresponding SERS performances, as shown in Fig. 2 (in the text), it was found that higher contents of Cl with higher binding energies may be responsible for the observations of stronger SERS effects from the viewpoint of CHEM enhancement since the SERS effect chiefly comes from the corresponding complex formed at the interface of roughened metal.[4]

References

1 Y. C. Liu, *Langmuir,* 2002, **18**, 174.
2 K. H. Yang, Y. C. Liu and C. C. Yu, *J. Mater. Chem.*, 2008, **18**, 4849.
3 E. Hesse and J. A. Creighton, *Langmuir*, 1999, **15**, 3545.
4 M. Baibarac, L. Mihut, G. Louarn, J. Y. Mevellec, J. Wery, S. Lefrant and I. Baltog, *J. Raman Spectrosc.*, 1999, **30**, 1105.
5 P. Gao, M. L. Patterson, M. A. Tadayyoni and M. Weaver, J. *Langmuir*, 1985, **1**, 173.
6 T. E. Furtak and D. Roy, *Surf. Sci.*, 1985, **158**, 126.
7 M. C. Henry, C. C. Hsueh, B. P. Timko and M. S. Freund, *J. Electrochem. Soc.,* 2001, **148**, D155.